3-3-2012

Phosphatidylserine Colocalizes With Epichromatin In Interphase Nuclei And Mitotic Chromosomes

Igor Prudovsky

Calvin P.H. Vary

Yolanda Markaki

Ada L. Olins

Donald E. Olins

Nucleus

ISSN: 1949-1034 (Print) 1949-1042 (Online) Journal homepage: https://www.tandfonline.com/loi/kncl20

Phosphatidylserine colocalizes with epichromatin in interphase nuclei and mitotic chromosomes

Igor Prudovsky, Calvin P.H. Vary, Yolanda Markaki, Ada L. Olins & Donald E. Olins

To cite this article: Igor Prudovsky, Calvin P.H. Vary, Yolanda Markaki, Ada L. Olins & Donald E. Olins (2012) Phosphatidylserine colocalizes with epichromatin in interphase nuclei and mitotic chromosomes, Nucleus, 3:2, 200-210, DOI: 10.4161/nucl.19662

To link to this article: https://doi.org/10.4161/nucl.19662

Nucleus 3:2, 200–210; March/April 2012; © 2012 Landes Bioscience

Phosphatidylserine colocalizes with epichromatin in interphase nuclei and mitotic chromosomes

Igor Prudovsky,[1] Calvin P.H. Vary,[1] Yolanda Markaki,[2] Ada L. Olins[3] and Donald E. Olins[3,*]

[1]Maine Medical Center Research Institute; Scarborough, ME USA; [2]Department of Biology II; Ludwig Maximilians University; Munich, Germany; [3]Department of Pharmaceutical Sciences; College of Pharmacy; University of New England; Portland, ME USA

Keywords: nuclear architecture, glycerophospholipid, chromatin, confocal and deconvolution microscopy

Abbreviations: PS, phosphatidylserine; PC, phosphatidylcholine; PFA, formaldehyde; NE, nuclear envelope; INM, inner nuclear membrane; 3D-SIM, structured illumination microscopy; PLC(D), phospholipase C(D)

Cycling eukaryotic cells rapidly re-establish the nuclear envelope and internal architecture following mitosis. Studies with a specific anti-nucleosome antibody recently demonstrated that the surface ("epichromatin") of interphase and mitotic chromatin possesses a unique and conserved conformation, suggesting a role in postmitotic nuclear reformation. Here we present evidence showing that the anionic glycerophospholipid phosphatidylserine is specifically located in epichromatin throughout the cell cycle and is associated with nucleosome core histones. This suggests that chromatin bound phosphatidylserine may function as a nucleation site for the binding of ER and re-establishment of the nuclear envelope.

Introduction

Peripheral chromatin, located adjacent to the inner nuclear membrane (INM) of the interphase nucleus, is immunologically distinct from internal chromatin when examined with a specific autoimmune mouse monoclonal antibody (PL2-6) directed against a conformational epitope within the nucleosome.[1,2] Furthermore, mitotic chromosomes exhibit surface staining with PL2-6, even though the nuclear envelope (NE) is no longer present during "open" mitosis. We have named this distinctive surface region "epichromatin" and hypothesized that it represents a chromatin conformation which persists through mitosis, facilitating postmitotic nuclear envelope reformation and the re-establishment of interphase nuclear architecture.[2] The structure and mechanism of formation of the epichromatin epitope remain largely unknown, although histones H2A, H2B and DNA are likely involved.[1] Localization of epichromatin in proximity to the INM suggests that it may contain bound phospholipids. Phosphatidylserine (PS) is the major anionic glycerophospholipid within eukaryotic membranes, being distributed asymmetrically within lipid bilayers and involved in binding to membrane associated polycationic proteins.[3] During apoptosis, PS is externalized at the plasma membrane, where it can be detected with Annexin V or a PS-specific monoclonal antibody (1H6).[4-6] PS has also been detected at the nucleoplasmic side of the NE with GFP-Annexin V, where it is likely derived from continuity of the NE with the ER.[7] In the present study, we demonstrate by immunostaining that PS is localized within the epichromatin region of interphase nuclei and mitotic chromosomes, exhibiting a location which is conserved in evolution.

Results

Immunofluorescent analysis of nuclear phosphatidylserine localization. In order to examine the distribution of chromatin-associated phosphatidylserine during the division cycle, we performed an immunostaining comparison of anti-PS antibody (1H6) with anti-epichromatin antibody (PL2-6) on rapidly growing tissue culture cells (i.e., human U2OS and mouse NIH 3T3). With the use of 1H6 on formaldehyde-fixed (PFA) and Triton X-100 permeabilized U2OS cells, the deconvolution microscopy images (**Fig. 1A–F**) bore a remarkable resemblance to U2OS cells immunostained with anti-epichromatin PL2-6 (ref. 2, **Fig. 2A**). For both antibodies, the interphase nuclei showed strong staining adjacent to the INM. During prophase, 1H6 staining was apparent on the most peripheral chromosomal regions, while at metaphase it surrounded the congressed chromosomes. During early anaphase, 1H6 reactivity remained confined to the periphery of chromosomes, whereas by late anaphase it was detectable on trailing chromosome arms. During telophase and G1 phase, the decondensing chromosomes showed only peripheral surface staining, similar to results for interphase epichromatin. We have obtained identical images using 1H6 on U2OS cells fixed with methanol (-20°C, 10 min), indicating that the fixation reagent is not a factor. In addition, we have recently identified a second independently derived purified mouse monoclonal anti-phosphatidylserine (Abcam clone 4B6), which yields identical immunofluorescent staining, compared with 1H6, with either PFA or ethanol fixation (**Fig. S1**). A more direct demonstration of colocalization of PS within the epichromatin region is presented in **Figure 1G–I**. Interphase and mitotic chromosomes

*Correspondence to: Donald E. Olins; Email: dolins@une.edu
Submitted: 12/08/11; Revised: 02/04/12; Accepted: 02/08/12
http://dx.doi.org/10.4161/nucl.19662

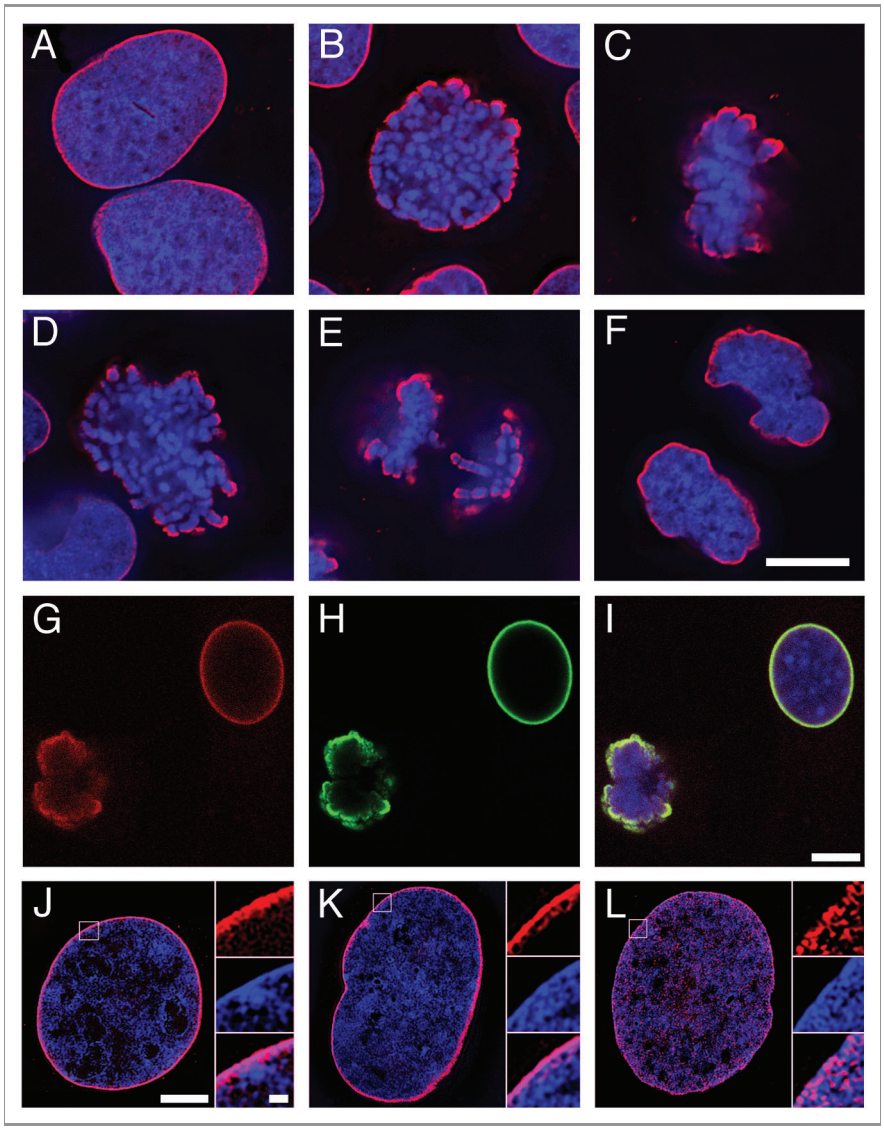

Figure 1. Immunostaining of interphase and mitotic cells with anti-phosphatidylserine (1H6) compared with epichromatin (PL2–6). (A–F) Deconvolution imaging of PFA-fixed U2OS cells with 1H6 (red) and DAPI (blue). (G–I) Confocal images of colocalized 1H6 (red) and PL2–6 (green) on methanol-fixed NIH 3T3 cells; blue represents TOPRO-3 stained DNA. Images are merged in (I). (J–L) 3-D SIM images of PFA-fixed U2OS cells reacted with 1H6 (J), PL2–6 (K) and PL2–7 (L); antibodies staining (red), DAPI (blue). Higher magnification inserts are shown at the right of each frame, presented top-to-bottom as antibody, DAPI and merge. Scale bars: (A–F), 10 μm; (G–I), 10 μm; (J–L), 5 μm; (J–L inserts), 500 nm.

of methanol-fixed NIH 3T3 cells were reacted first with PL2-6, washed with PBS and reacted with FITC-anti-mouse IgG. Subsequent PBS washes were followed by incubation with an excess of normal mouse IgG, in order to saturate all binding sites on the anti-mouse IgG. Lastly, the slides were incubated with TRITC-1H6, washed, incubated with TOPRO-3 and visualized by confocal microscopy. Supporting images document that the peripheral staining by 1H6 is not a consequence of an antibody-established barrier against diffusion (**Fig. S2A**). For immunostaining, we normally employ 1H6 at 1:200 dilution; identical, but weaker, images are obtained up to a 1:5400 dilution, making it unlikely that a concentration-dependent "layer" of bound antibody impedes diffusion of 1H6 deeper into the nucleus. A related control experiment (**Fig. S2B**) demonstrates that there is neither a 1H6 barrier blocking the nuclear penetration of an unrelated mouse mAb (BM28), nor does the strong peripheral FITC staining cause any obvious attenuation of the exciting and emitted light.

Employing 3D Structured Illumination Microscopy (3D-SIM),[8] we have obtained high resolution immunostaining images (**Fig. 1J–L**) of interphase U2OS cells reacted with 1H6, PL2-6 and PL2-7 (an independent monoclonal anti-nucleosome antibody obtained from the same mouse as PL2-6).[2] Both 1H6 and PL2-6 stained a thin rim at the periphery of the DAPI-stained DNA, while PL2-7 reacted throughout the chromatin. The similarity of staining in the epichromatin region by both 1H6 and PL2-6 (but not PL2-7) throughout the cell cycle is dramatically demonstrated with single 3D-SIM slices (**Fig. 2**).

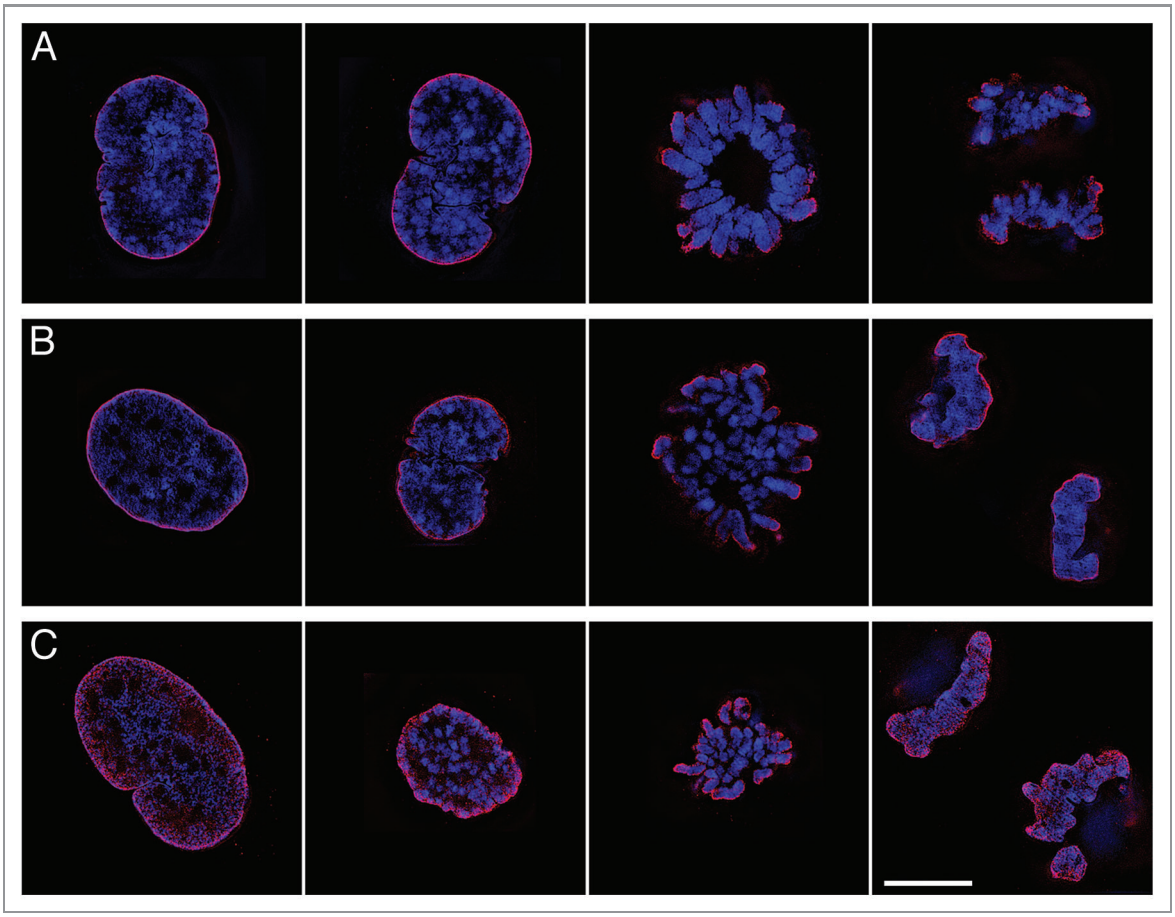

Figure 2. 3-D SIM images of immunostained U2OS cells throughout the cell cycle. (A) 1H6 (red) and DAPI (blue). (B) PL2-6 (red) and DAPI (blue). (C) PL2-7 (red) and DAPI (blue). Each row is a gallery of single optical slices with the same antibody. Columns (left to right): interphase; prophase; metaphase; late anaphase-telophase. Note the peripheral staining by 1H6 and PL2-6, and the deep nuclear staining of PL2-7. Scale bar: 10 μm.

Co-immunostaining comparisons of 1H6 with other nuclear antibodies are presented in **Figure 3**. A single U2OS nucleus co-stained with 1H6, anti-lamin B and DAPI and imaged by 3D-SIM is shown (**Fig. 3A–C**). Examination of the nuclear envelope at higher magnification (**Fig. 3C**, insert), demonstrated that lamin B is exterior to 1H6 staining (see also, **Figure 4**). The images also show that the nucleoplasmic reticulum[9] is stained by anti-lamin B (arrows), but not by 1H6 (also not stained with PL2-6).[2] Employing deconvolution microscopy to examine co-immunostained mitotic chromosomes, compared with 1H6, we found that: (1) the "mitotic marker" anti-H3S10p is present at the surface of metaphase chromosomes, penetrating more deeply into the chromosomes than 1H6 (**Fig. 3D–F**); (2) the INM protein lamin B receptor (LBR) is retained within the cytoplasm, while 1H6 binds at mitotic chromosome outer surfaces (**Fig. 3G–I**) and (3) the INM protein emerin is distributed in a similar manner to LBR (**Fig. 3J–L**). Identical colocalization images comparing PL2–6 with H3S10p, LBR and emerin in U2OS cells have been published earlier (**Figs. 3 and 4**).[2]

Association of the phosphatidylserine epitope with compacted interphase peripheral chromatin. It has long been known that exposure of live tissue culture cells to hypertonic (hyperosmotic) buffer conditions rapidly leads to interphase chromatin condensation resembling the beginning of prophase.[10] Presently, this induction of compacted interphase chromatin is regarded as an example of macromolecular crowding (volume exclusion), rather than the induction of mitosis.[11] A recent study clearly demonstrated, by fluorescence microscopy and thin section electron microscopy, that treatment of MCF7 cells with a hypertonic buffer (320 mM sucrose added to tissue culture medium) for about 20 min induced compaction of peripheral chromatin, which moved away (retracted) from the still intact interphase nuclear envelope, generating "lacunas of fine fibrillar material."[12] We decided to expose U2OS cells to the same hypertonic conditions, followed by formaldehyde fixation and immunostaining with 1H6 and PL2-6, to see whether the PS and epichromatin epitopes remained at the nuclear envelope or retracted with the compacted peripheral chromatin (**Fig. 4**). Using deconvolution microscopy, the resulting images convincingly demonstrated that both epitopes remained associated with the retracted chromatin in the epichromatin region. With respect to PS localization, this experiment strongly argues that its interaction with peripheral chromatin is much stronger than its interaction with other lipids of the INM.

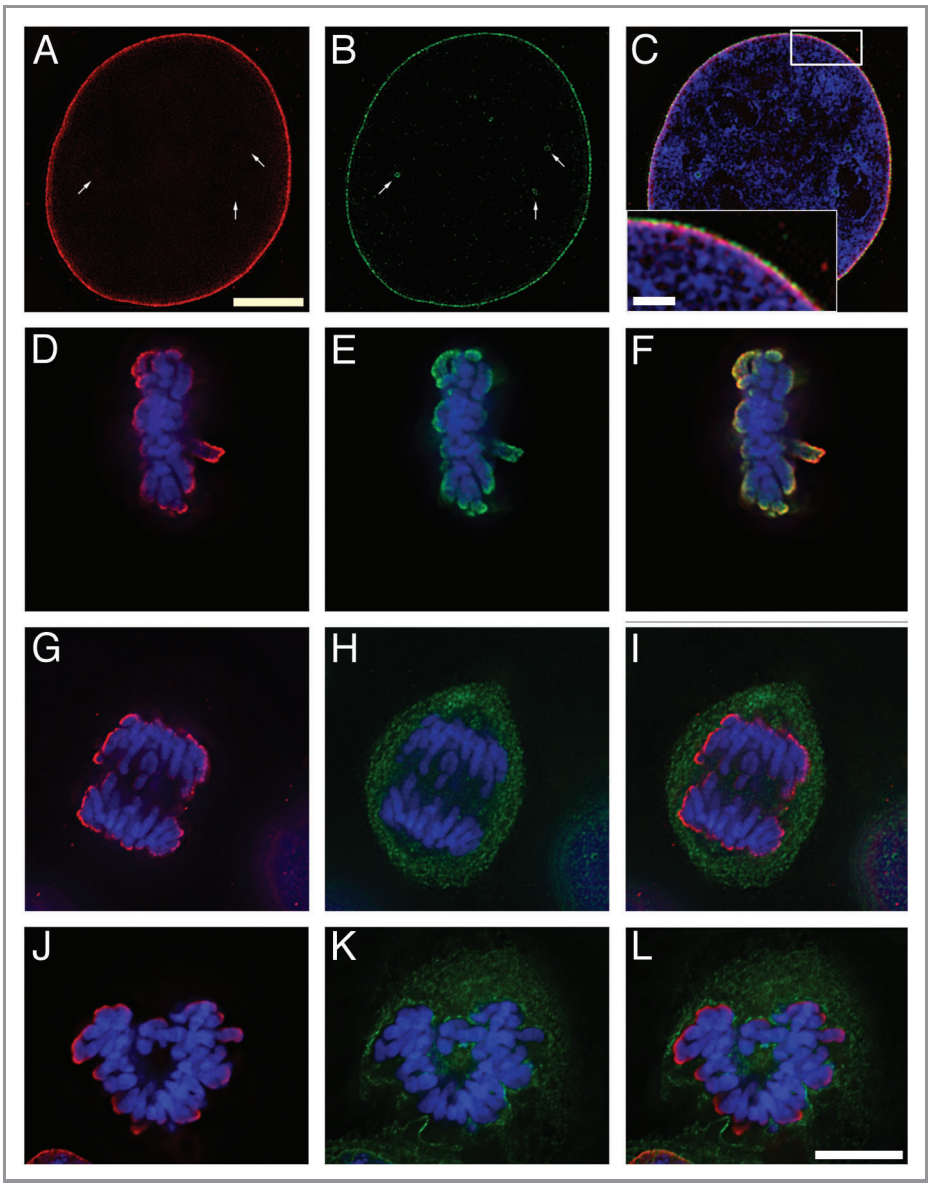

Figure 3. Immunostaining of interphase and mitotic cells with anti-phosphatidylserine (1H6) compared with other anti-nuclear antibodies. (A–C) 3-D SIM of a single U2OS nucleus stained with 1H6 (red), anti-lamin B (green), DAPI (blue); merged (C); insert in (C), higher magnification of nuclear envelope staining. Arrows indicate cross-sections of nucleoplasmic reticulum, not stained with 1H6. (D–F) Deconvolution microscopy of congressed mitotic chromosomes in U2OS cells co-immunostained with 1H6 (red), the "mitotic marker" anti-H3S10p (green) and DAPI (blue); merged (F). (G–I) Deconvolution images of late anaphase U2OS mitotic chromosomes co-immunostained with 1H6 (red), anti-LBR (green) and DAPI; merged (I). (J–L) Deconvolution images of metaphase U2OS chromosomes co-immunostained with 1H6 (red), anti-emerin (green) and DAPI (blue); merged (L). Scale bars: (A–C), 5 μm; insert in (C), 1 μm; (D–L), 10 μm.

Conserved location of chromatin-associated phosphatidylserine. *Drosophila melanogaster*, like most eukaryotes, possesses PS in its cellular membranes.[3] The evolutionary conservation of PL2-6 staining has been demonstrated in diverse animal and plant species.[2] To examine whether the 1H6 epitope is also conserved, we immunostained Drosophila Kc cells with 1H6 or PL2-6 combined with the mitotic marker, anti-H3S10p, using deconvolution microscopy to view interphase and mitotic cells. **Figure 5** demonstrates that PL2-6 and 1H6 yield identical and highly conserved staining patterns, similar to immunostained mammalian cells.

Characterizing the differences between 1H6 and PL2-6. Given the apparent identity of immunostaining by 1H6 and PL2-6, we attempted to distinguish the epitopes recognized by these two purified monoclonal antibodies of independent origins; the immunogen of 1H6 being liposomes containing PS, whereas PL2-6 is derived from an autoimmune mouse. Toward this goal, 1H6 and PL2-6 were absorbed with three types of liposome suspensions in PBS, separately prepared from PS, PC (phosphatidylcholine) or a combination of PS + PC (50:50 mixture), prior to immunostaining ethanol-fixed NIH 3T3 cells (**Fig. 6A**). The results demonstrated that absorption by PS significantly reduces

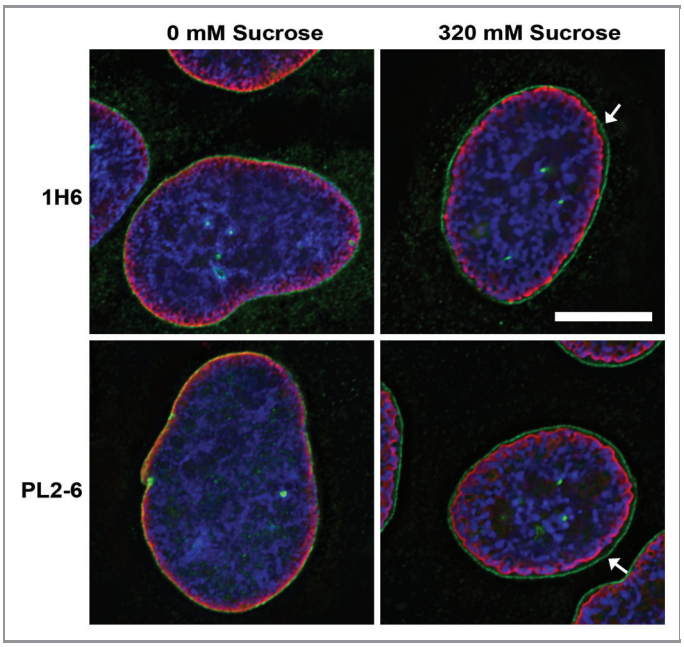

Figure 4. Effect of hypertonic treatment of live U2OS cells on subsequent immunostaining by anti-phosphatidylserine (1H6) and anti-epichromatin (PL2-6). Deconvolution images are presented. Columns: 0 mM sucrose; 320 mM sucrose (added to tissue culture medium). All images are merged. Top row: 1H6 (red); anti-emerin (green) and DAPI (blue). Bottom row: PL2-6 (red); anti-lamin A (green) and DAPI (blue). The arrows in the 320 mM sucrose images point to gaps between the nuclear envelope and the compacted chromatin. Scale bar: 10 μm.

the staining with 1H6, but not with PL2-6; absorption by PC had a negligible effect. The liposome suspension containing both phospholipids was also effective in absorbing 1H6, but not PL2-6. This strongly argues that PL2-6 does not interact with PS-containing liposomes. We also examined whether PL2-6 can bind to PS which has been coated onto an ELISA plate (**Fig. 6B**). The experiment clearly indicated that whereas 1H6 reacted with PS-coated wells neither normal mouse IgG nor PL2-6 showed more than negligible reactivity.

In order to further define the PS epitope present within the fixed cells, we performed two types of extractions on coverslip-attached NIH 3T3 cells. Ethanol-fixed cells were incubated with chloroform overnight at -20°C. Following chloroform extraction, the coverslips were washed in PBS and blocked with BSA/PBS prior to immunostaining. 1H6 gave negligible staining, PL2-6 was moderately reduced and BM28 (an unrelated MCM nuclear protein) was unaffected by exposure to chloroform (**Fig. 7A**). The reduction of PL2-6 staining may reflect perturbation of the epichromatin conformational epitope, but was clearly not as profound as the reduction of 1H6 staining. For the second type of extraction experiment, we attempted selective removal of histones from methanol-fixed NIH 3T3 cells by incubation of the coverslips with various NaCl concentrations in 20 mM Tris, pH 7.4 (0.6 M NaCl has been shown to extract H1 histone from chromatin; 1.2 M NaCl removes H2A and H2B).[13] Immunostaining demonstrated that PL2-6 staining was unaffected by 0.6 M NaCl extraction, whereas 1H6 staining was strikingly reduced (**Fig. 7B**). After incubation with 1.2 M NaCl, both

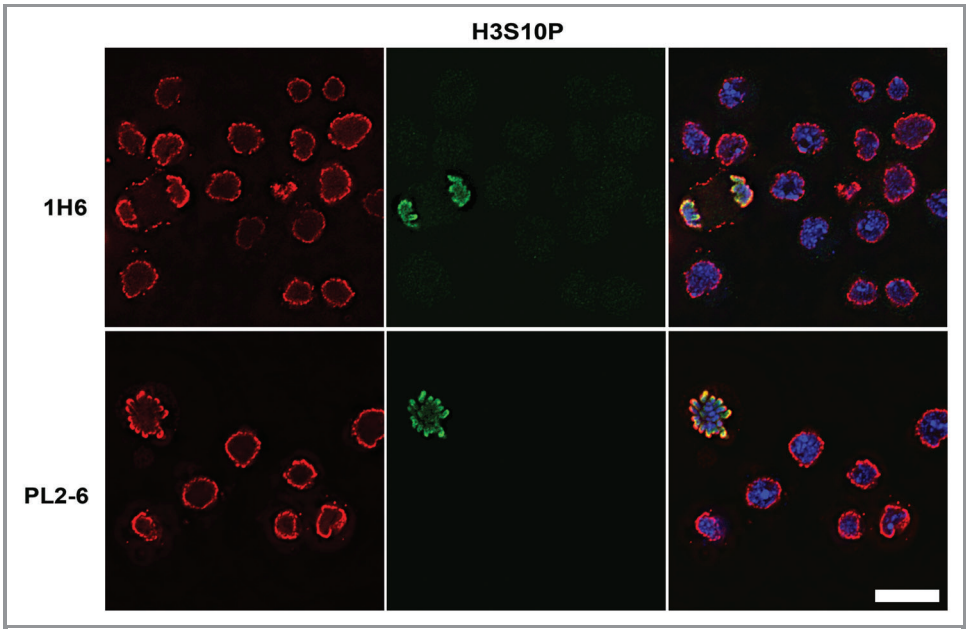

Figure 5. Anti-phosphatidylserine (1H6) and anti-epichromatin (PL2-6) staining of Drosophila Kc cells. Deconvolution images are presented. Top row, co-immunostaining with 1H6 (red), anti-H3S10p (green) and DAPI (blue); bottom row, co-immunostaining with PL2-6 (red), anti-H3S10p (green) and DAPI (blue). Right column, merged images. Scale bar: 10 μm.

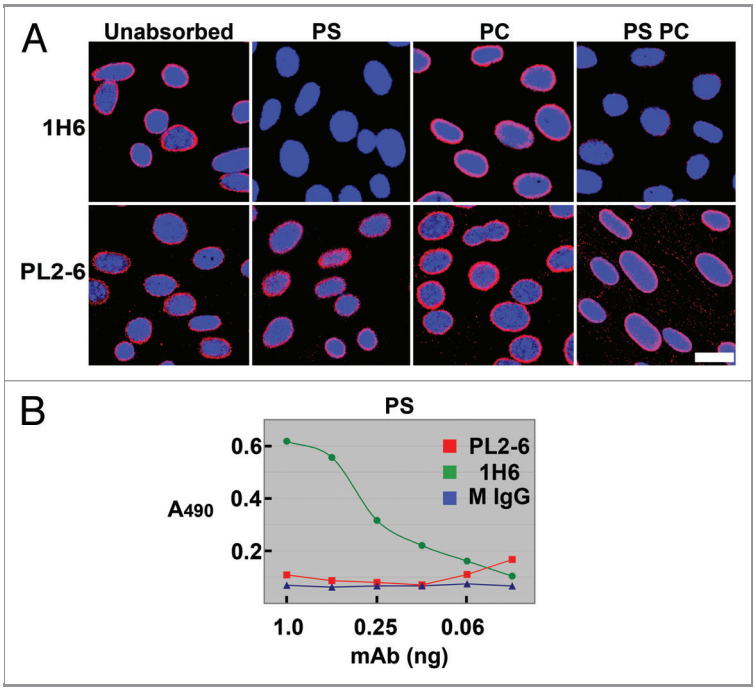

Figure 6. (A) Comparison of anti-phosphatidylserine (1H6) and anti-epichromatin (PL2-6) after absorption with PS, followed by immunostaining. Confocal images of NIH 3T3 cells immunostained with unabsorbed antibodies or after absorption with phosphatidylserine (PS), phosphatidycholine (PC) or a 50/50 mixture (PS PC). Image rows: top, 1H6; bottom, PL2-6. Color scheme: antibodies, red; TOPRO-3, blue. Scale bar: 20 μm. (B) ELISA comparison of PL2-6, 1H6 and normal mouse IgG (M IgG) binding to PS-coated wells. Y-axis: A_{490} from bound HRP anti-mouse IgG.

antibodies yielded minimal staining. Taken together, these two experiments imply that the epitopes, as present on fixed NIH 3T3 cells, can be distinguished by their different sensitivities to extraction; the PS epitope is more readily extracted by chloroform or NaCl, than is the epichromatin epitope.

Comparing the binding of 1H6 and PL2-6 to histones. In a series of experiments, we compared 1H6 and PL2-6 binding to histones using electrophoretic immunoblotting. Previously, we demonstrated that PL2-6 reacts with the "inner histones" (especially with H2A and H2B) by immunoblotting or "dot" blotting onto PVDF membranes.[2] When both 1H6 and PL2-6 were tested on PVDF membranes containing immunoblotted total acid-extracted histones[14] resolved by SDS-PAGE, they unexpectedly yielded similar patterns of interaction with histones (**Fig. 8A and B**, lanes M). These membrane strips had been blocked with 5% low fat milk powder in TBST. Subsequently, we learned that milk contains histones and DNA[15] and PS.[16] Therefore, we examined the influence of blocking buffer composition on the reactions of 1H6 and PL2-6 with acid-extracted histones. The results (**Fig. 8A and B**) clearly indicated that the reactions of both antibodies with H1 were augmented by milk. The reaction of PL2-6 with inner histones did not depend upon blocking with milk; but the 1H6 reaction with inner histones was considerably strengthened by milk. In a separate experiment (**Fig. 8C**), following milk blocking, treatment of membrane strips with phospholipase C or D strongly reduced subsequent reactivity with 1H6, arguing that PS in milk associates with histones bound to PVDF, resulting in significant 1H6 binding. In conclusion, when "properly" blocked (e.g., casein or BSA in TBST), 1H6 displays negligible reactivity with acid-extracted histones separated by SDS-PAGE and blotted onto PVDF membranes; whereas, PL2-6 reacts with inner histones (probably H2A and H2B), but exhibits negligible reaction with H1.

We considered the possibility that SDS-PAGE separation of the acid-extracted histones might destroy conformational epitopes recognized by either 1H6 or PL2-6. Therefore, we prepared histone subfractions from NIH 3T3 cells by a method which better preserves conformations within histone complexes.[17] ELISA assays were employed to compare the binding of 1H6 and PL2–6 to plates coated with the histone subfractions (H1, H2A + H2B and H3 + H4) extracted using an Active Motif kit, based upon.[17] The subfractions were also examined for "purity" on a 15% SDS-PAGE and stained with Coomassie blue (**Fig. S3**). Three different concentrations (1.0, 0.1 and 0.01 μg/ml) of monoclonal antibodies and normal mouse IgG were tested on the histone-coated ELISA plates after blocking with 0.5% casein in TBST (**Fig. 8D**). The results demonstrated that PL2-6 yielded strong reactions with H2A + H2B and H3 + H4. 1H6 exhibited clear reactions with the same histone subfractions (although the reaction with H3 + H4 was obviously more antibody concentration-dependent than with PL2-6). Thus, 1H6 recognizes H2A + H2B by ELISA, but exhibits only weak reactivity on immunoblots of SDS-PAGE resolved histones (**Fig. 8A**). **Figure 8E** shows that ELISA wells coated with H2A + H2B and subsequently digested with phospholipase C or D revealed significantly reduced reactivity with 1H6, suggesting that PS may be bound to this histone subfraction. The reaction of PL2-6 with H3+H4 (**Fig. 8D**) was also unexpected, given prior ELISA experiments with purified individual histones mixed in PBS to form histone complexes.[18] These results strongly suggest that the epichromatin epitope (PL2-6) and possible PS binding to histones (1H6) are better preserved in the Active Motif subfractions, compared with the histone complexes mixed in PBS.

In one final attempt to define possible interactions of 1H6 and PL2-6 with "extracted" histones, we combined mass spectroscopy with immunoprecipitation by 1H6 or PL2-6, using the "nuclear protein fraction" (Qproteome Cell Compartment Kit) from NIH 3T3 cells. By sequential incubation of cells with the kit proprietary extraction buffers, total nuclear proteins can be effectively separated from cytosolic, membrane and cytoskeletal proteins. The histones and other nuclear proteins are present in one fraction. Benzonase endonuclease treatment degrades the DNA to oligonucleotides, liberating the nuclear proteins. Immunoprecipitation with 1H6 or PL2-6 should trap histones and histone complexes. Normal mouse IgG was also employed for a "control" immunoprecipitation; common peptides observed with antibody and with IgG were interpreted as non-specific interactions and ignored.

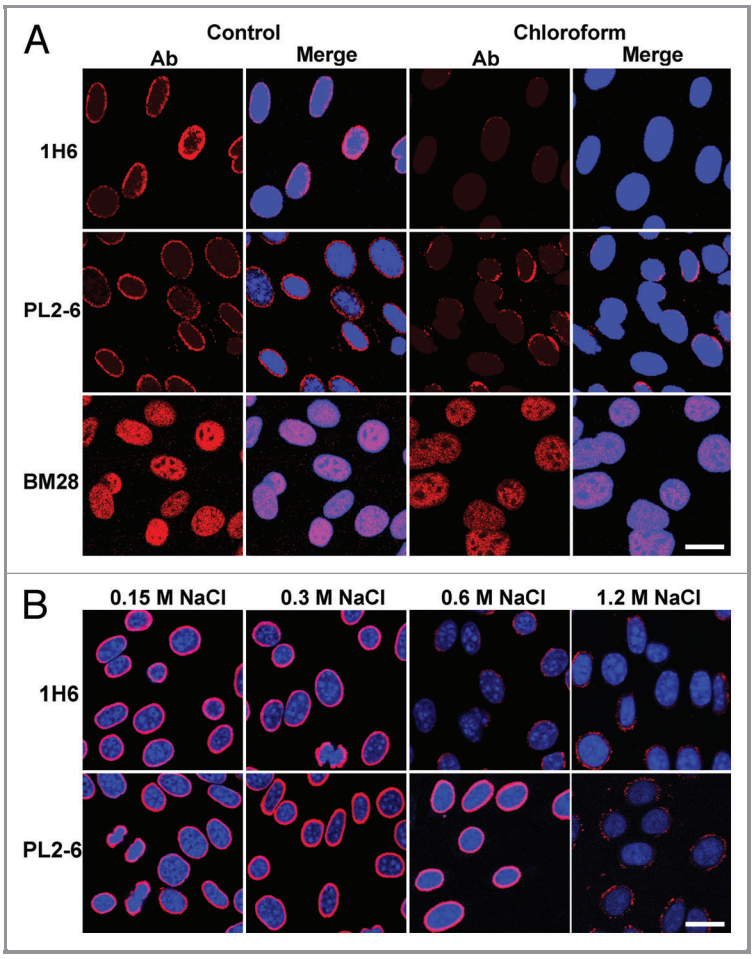

Figure 7. (A) Chloroform extraction of ethanol-fixed NIH 3T3 cells, prior to immunostaining and confocal imaging. Three mouse antibodies (1H6, PL2-6 and anti-BM28) were treated with ("Chloroform") or without prior extraction ("Control"). This experiment shows that the 1H6 epitope is extractable with chloroform. Color scheme: Ab, antibodies (red); DNA (blue) stained with TOPRO-3. Scale bar, 20 μm. (B) NaCl extraction of methanol-fixed NIH 3T3 cells prior to immunostaining and confocal imaging. Two mouse antibodies (red), PL2-6 and 1H6, were tested after NaCl extraction. TOPRO-3 (blue) was employed to stain DNA. Scale bar: 20 μm.

We obtained clear evidence that both antibodies 1H6 and PL2-6 can interact with inner histones in solution; whereas, only PL2-6 significantly precipitates H1 (**Fig. 8F**). Examples of identified representative histone peptide sequences are presented in **Figure S4**. This experiment identifies specific histones that were detected in the immunoprecipitates, but does not yield information on the quantities of the histones, whether they were part of a protein complex or whether (in the case of 1H6) there was bound phosphatidylserine. Collectively, the immunoblotting, ELISA and immunoprecipitation plus mass spectroscopy argue that 1H6 does interact with H2A + H2B. But it is likely that this interaction is mediated through PS bound to H2A or to the H2A + H2B dimer. However, the interaction of PL2-6 with the inner histones does not depend upon the presence of PS (see **Figs. 3B and 8B**).

Discussion

The present study provides evidence that PS colocalizes with epichromatin. We have documented that two independently derived and purified mouse monoclonal antibodies (1H6 and 4B6), developed by immunizing with liposomes containing PS[4,5] and used to detect apoptosis (comparable to PS-specific Annexin V), stain the surfaces of chromatin in an interphase nucleus and on mitotic chromosomes, a region also recognized by the mouse anti-nucleosome monoclonal antibody PL2-6.[2] Despite the similar immunostaining pattern of these mouse antibodies, they exhibit significant differences. Comparing 1H6 and PL2-6: (1) 1H6, but not PL2-6, can be absorbed by PS-containing liposomes, prior to immunostaining of ethanol-fixed NIH 3T3 cells. (2) By ELISA assay, 1H6 binds to PS, while PL2-6 does not. (3) Extraction of ethanol-fixed NIH 3T3 cells with chloroform depletes 1H6 immunostaining more effectively than PL2-6 staining. (4) NaCl extracts the 1H6 epitope from methanol-fixed NIH 3T3 cells at 0.6 M, with no reduction in PL2-6 staining. These observations strongly argue that 1H6 recognizes PS complexed with chromatin, while PL2-6 does not bind to PS.

There are very few studies on the consequences of glycerophospholipid interactions for chromatin structure and function. In a series of studies on isolated rat liver nuclei,[19-21] addition of PS but not PC, vesicles was shown to enhance DNase I sensitivity, facilitate production of mononucleosomes by micrococcal nuclease, extract histone H1 (but not inner histones) and stimulate endogenous RNA polymerase activity. Two other studies[22,23] focused on the strong electrostatic interactions of anionic phospholipids [PS and cardiolipin (CL)] with histones. By ELISA, the interaction of histones with CL was shown to be ionic strength dependent with strong binding at 0.3 and 0.6 M NaCl but severely reduced binding at 1.2 and 2.4 M NaCl.[22] With the use of surface plasmon resonance, histone H2A has the highest association constant with PS-containing vesicles compared with the other individual histones.[23] The authors suggest that the binding of histones to phospholipids "may contribute to the binding of histones to surfaces and blebs of apoptotic cells." This conclusion is supported by recent evidence that H2B is tethered at the surface of macrophage and apoptotic cells via electrostatic interactions with PS.[24]

From the present and prior[18] studies, there is little doubt that PL2-6 recognizes histones, principally the inner histones H2A and H2B. It is less clear whether 1H6 can bind histones independently of the presence of PS. The present immunoblotting and ELISA experiments strongly indicate that reactions of 1H6 with histones or histone complexes are significantly reduced by treatment with phospholipases C and D prior to the immunoassay. It remains possible that 1H6 may be directed against an epitope consisting of PS plus histone amino acid residues. Such multireactive antibodies are not rare in autoimmunity and are

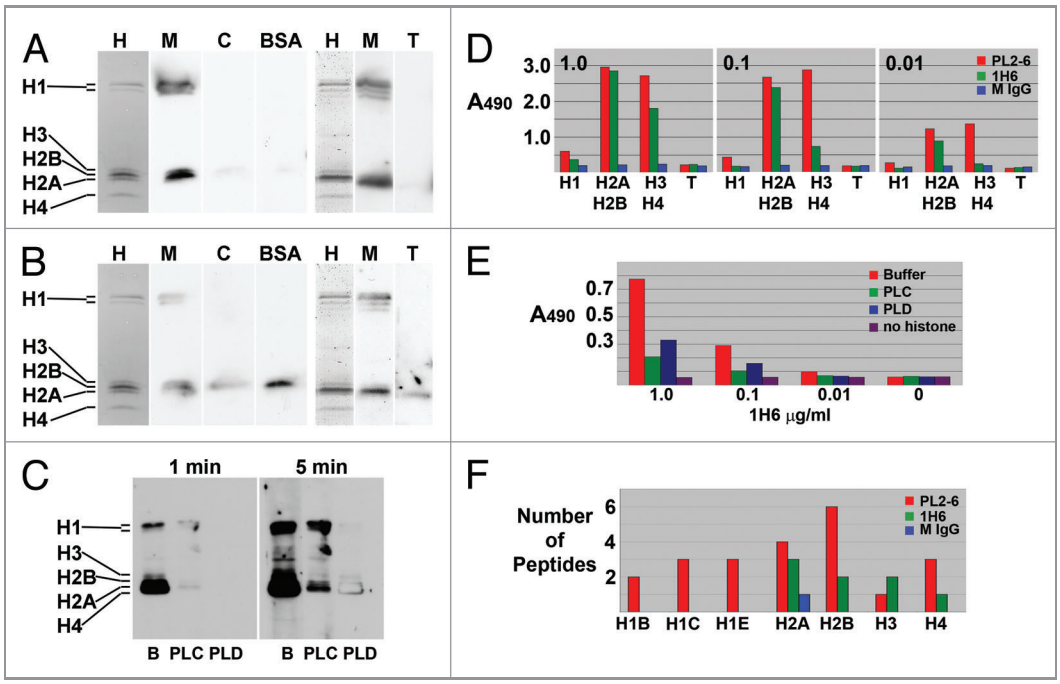

Figure 8. Immunochemical comparisons of anti-phosphatidylserine (1H6) and anti-epichromatin (PL2-6). (A) Effect of different blocking agents on PVDF immunoblots of acid extracted histones from HL-60/S4 cells reacted with anti-phosphatidylserine (1H6): H, Ponceau S stained histones; M, 5% milk/TBST; C, 1% casein/TBST; BSA, 5% BSA/TBST; T, TBST. (B) Equivalent PVDF immunoblots reacted with anti-epichromatin (PL2-6). (C) Effects of phospholipase C (PLC), phospholipase D (PLD) or digestion buffer (B) upon PVDF immunoblots of acid extracted histones, after blocking with 5% milk/TBST. ECL exposure times (same blot): 1 and 5 min. (D) ELISA comparison of PL2-6, 1H6 and normal mouse IgG (M IgG) binding to NIH 3T3 histone subfractions (H1, H2A +H2B, H3+H4) and TBST control (T). The antibodies and IgG were tested at three concentrations: 1.0, 0.1 and 0.01 μg protein/ml. Y-axis: A_{490} from bound HRP anti-mouse IgG. (E) ELISA comparison of H2A+H2B subfraction treated with phospholipase (PL) C or D, reacted with dilutions of 1H6. Y-axis: A_{490} from bound HRP anti-mouse IgG. (F) Mass spectroscopic analyses of immunoprecipitated nuclear proteins from NIH 3T3 cells. The bar graph indicates the number of distinct peptides (> 95% confidence) used to identify the indicated histones, based upon reactions with 1H6 and PL2-6, compared with normal mouse IgG (M IgG). H2A- and H2B-derived peptides comprised the largest fraction of total spectra obtained, as reflected in the peptide counts.

currently viewed as a consequence of exposed nucleosome determinants at the cell surface of apoptotic cells.[25]

An unresolved puzzle is why 1H6 can recognize PS in the epichromatin region and when exposed in apoptosis but does not detect PS in other cellular membranes. From analytical cell fractionation studies,[3,26] PS is present in measurable quantities in the ER, Golgi and the plasma membrane. When GFP-lactadherin C2 domain was expressed in various tissue culture cell lines (A431, BHK-21, HeLa, COS7) PS was detected at the cytoplasmic side of the plasma membrane, the Golgi and endocytic vesicles and at the luminal side in ER and Golgi.[27] GFP-Annexin V was transfected into Neuro 2A cells and internal calcium levels elevated by treatment with ionomycin, leading to detection of PS "in the cytoplasmic leaflet of the plasma membrane and possibly in the nucleoplasmic face of the nuclear envelope."[7] The lack of detection by 1H6 of PS in these various cell membranes might be due to, at least, three causes. The fixation procedures may lead to a selective loss of PS from most cellular membranes,[28] sparing the PS associated with epichromatin. Second, the PS epitope recognized by 1H6 may be "masked" in most membranes. Third, the PS epitope recognized by 1H6 may be different in its presentation when bound to histones or chromatin, as in apoptotic bodies and in the nucleus, than when present in most membranes.

When interphase chromatin is compacted by hypertonic sucrose (320 mM), the epitopes for both 1H6 and PL2-6 remain associated with the chromatin surface, clearly showing that they can be separated from the inner nuclear envelope membrane. This experiment also indicates that induced chromatin retraction does not result in a random redistribution of chromatin-bound PS; i.e., PS is tightly associated with the epichromatin region. However, we cannot rule out the possibility of PS redistribution from membranes specifically to the epichromatin region during the fixation and permeabilization protocols needed for immunofluorescent staining.

Nuclear envelope breakdown and reformation during mitosis must reproduce a faithful rendition of the parental nucleus in the derived daughter cells.[29,30] An important question is how epichromatin might play a role in directing postmitotic reformation. Persistence of the epichromatin epitope throughout mitosis elicited the hypothesis[2] that the surface of interphase and mitotic chromatin possesses a conformation which facilitates attachment of NE components. The present study suggests that phosphatidylserine from the interphase inner nuclear membrane may remain attached to epichromatin during mitosis, functioning as "nucleation sites" for the binding of ER and the re-establishment of the NE during postmitotic nuclear reformation.

Materials and Methods

Cell lines. Human U2OS cells were cultivated in DMEM medium, plus 20% fetal calf serum and 2 mM L-glutamine. Human HL-60/S4 suspension cells were maintained in RMPI 1640 medium, plus 10% heated fetal calf serum and 2 mM L-glutamine. Mouse NIH 3T3 cells (ATCC, Manassas VA) were maintained in DMEM, plus 10% calf serum. *Drosophila melanogaster* Kc 167 cells were maintained at 25°C, in Schneider's Drosophila medium supplemented with 10% heated fetal calf serum. All cultures contained Pen/Strep. HL-60/S4 cells were harvested for microscopy at a concentration of ~10^6 /ml; coverslip attached U2OS and Drosophila Kc cells were used prior to confluence. For confocal imaging, NIH 3T3 cells were plated on fibronectin-coated glass coverslips.

Antibodies. The sources and use of mouse monoclonal PL2-6, PL2-7, rabbit anti-H3S10p, guinea pig anti-LBR and guinea pig anti-emerin have been described earlier.[2] PL2-6 and PL2-7 were purified from tissue culture supernatants by affinity chromatography on protein G-Sepharose columns.[18] 1H6 and TRITC-1H6 was purchased from Millipore. The immunogen for 1H6 was liposomes containing 70% phosphatidylserine and 30% phosphatidylglycerol. For colocalization experiments, 1H6 was labeled with TRITC using fluoreporter protein labelling kit (Life Technologies). A second purified mouse monoclonal anti-phosphatidylserine (Abcam clone #4B6) was examined, based upon a published use of this antibody for immunostaining.[31] Mouse monoclonal anti-BM28 is from Transduction Laboratories. Goat anti-lamin B is from Santa Cruz Biotechnology. Normal mouse IgG was obtained from Sigma Aldrich. For immunostaining experiments the mouse monoclonal antibodies were used at ~5–10 μg/ml; immunoblots were performed ~0.5–1.0 μg/ml.

Immunostaining. A number of different protocols were employed, following slightly different methods in the different laboratories using different microscopes. When employing the DeltaVision deconvolution microscope at the German Cancer Research Center, PFA (formaldehyde) fixation, permeabilization and visualization were as described earlier for the study of U2OS, HL60/S4 and Drosophila Kc cells.[2] Confocal data collected on NIH 3T3 cells using a Leica SP1 microscope (Maine Medical Center Research Institute) employed methanol or ethanol fixation (-20°C, 10 min), with DNA stained by TOPRO-3 and mounted in Vectashield. For the colocalization experiment (confocal imaging), PL2-6 was reacted first, followed by FITC-anti-mouse IgG, an excess of normal mouse IgG and, finally, TRITC-1H6. Besides demonstrating colocalization of the two mAbs, this experiment demonstrated that prior binding by PL2-6 did not significantly inhibit1H6.

Samples prepared for 3-D SIM analysis (University of Munich) followed a protocol similar to the earlier publication,[2] with the following differences: 2% PFA/PBS, 10 min, RT; gradient exchange from fixative to 0.02% Tween 20/PBS; 20 mM glycine/PBS, 10 min; 0.5% Triton X-100/PBS, 10 min; blocking with 2% BSA, 0.5% fish skin gelatin, 0.1% Tween 20/PBS; primary and secondary antibodies dissolved in blocking buffer; 4 washes in blocking buffer; post-fixation in 4% PFA/PBS; gradient buffer exchange (as above); DAPI staining and washing in PBS; mounting in Vectashield. Regardless of the specific fluorophor conjugated to the secondary antibody, images of 1H6 staining are artificially colored red in all figures. The other antibodies are presented in red or green, for convenience. DNA (chromatin) is artificially colored blue, regardless of whether the staining was with DAPI or TOPRO-3. All adjustments of brightness, contrast or color balance were linear adjustments and applied to the whole image.

Immunoblotting. Total acid extracted histones were prepared from undifferentiated HL-60/S4 cells following a published procedure.[14] Gradient (10–20%) SDS-PAGE (BioRad Criterion) was run at 200 V for 1hr. Each lane had acid extract from ~3×10^5 cells. Electrophoretic transfer to PVDF membrane was performed with a BioRad semidry apparatus in 250 mM glycine, 25 mM Tris, 0.05% SDS and no methanol, at 130 mA for 45 min. PVDF membranes were placed on both sides of the gel; each was stained with Ponceau S to confirm that histone migration was toward the anode. After the histone containing membrane was dry, it was cut into strips. For the blocking experiment, all strips were wetted with methanol, washed with TBST (Tris buffered saline + Tween 20) for 30 min, blocked with 5% milk in TBST, 1% casein (Sigma-Aldrich) in TBST, 5% BSA in TBST or TBST alone for 30 min at RT. Primary antibody dilutions (1H6 or PL2-6 in TBST) were incubated for 1 h at RT under parafilm strips.

Following 6 × 5 min TBST washes of each strip in separate Petri dishes, each strip was incubated in HRP-antimouse IgG (1:5000 dilution in TBST) 1 h at RT under fresh parafilm strips and washed 6 × 5 min in separate fresh Petri dishes with TBST. ECL and film exposure were as described earlier.[2] For testing the reactivity of 1H6 on the PVDF strips after milk blocking followed by phospholipase digestion, strips were incubated with 5% milk/TBST (1 h, 42°C), washed in TBST, followed by 25 mM Tris/HCl (pH 7.4), 140 mM NaCl, 2 mM CaCl2, then phospholipase C (PLC, 2.2 units/ml; Sigma P7633) or 50 mM Tris/HCl (pH 8.0), 140 mM NaCl, 5 mM CaCl2, containing phospholipase D (PLD, 3.8 units/ml; Sigma P0515) and incubated 1 h at 37°C. The strips were washed with TBST and incubated with 1H6. After washing with TBST, the strips were incubated in 5% milk (10 min, 37°C), then HRP conjugated 2° Ab (30 min), washed and developed with ECL for 1 and 5 min. This experiment argues that glycerophospholipids in milk (presumably PS) bind to blotted acid-extracted histones, leading to reactions with 1H6. Milk does not lead to nonspecific binding of the secondary antibody, only of 1H6.

ELISA. For analysis of the binding of 1H6, PL2–6 and normal mouse IgG to NIH 3T3 histone subfractions (H1, H2A+H2B and H3+H4), these fractions were diluted to 10 μg/ml in PBS. 50 μl of each sample was loaded per well on a PVC 96 well ELISA plate, covered with a sealing membrane and incubated ON at 4°C. Wells were washed three times with 100 μl TBST and blocked with 0.5% casein in TBST, 1 h at RT. 100 μl 1H6, PL2-6 or mouse IgG at 1.0, 0.1 and 0.01 μg/ml in TBST, or TBST alone, was added to each well and incubated 2 h at RT. Following

three washes with 200 µl TBST, 150 µl of HRP-antimouse IgG (1:5000 in TBST) was added for 1 h at RT. Following 4 × 200 µl TBST washes, OPD (o-phenyldiamine dihydrochloride) plus H_2O_2 in citrate buffer (pH 5.5) was added. Absorbance was read at 490 nm.

To examine the PS binding capability of 1H6, PL2–6 and normal mouse IgG, wells of a solid plastic immunoplate (Costar, #3798) were coated with 25 µl/well of PS (Avanti Polar Lipids) dissolved in hexane (20 µg/ml), which was allowed to evaporate ON at RT. Duplicate wells were blocked with 1% BSA in PBS for 2 h at RT, washed with 300 µl PBS, incubated with 25 µl of serial 2-fold dilutions of 1H6, PL2–6 or normal mouse IgG (starting at 1 µg protein/ml) in 1% BSA/ PBS and incubated 1 h at RT. Wells were washed with 5 × 300 µl PBS, followed by 25 µl HRP-anti-mouse IgG (1:7500) in 1% BSA/PBS for 1 h at RT, washed again with 8 × 300 µl PBS and treated with OPD plus H_2O_2 in citrate buffer, followed by reading at 490 nm. To examine the effect of PLC and PLD upon the H2A + H2B subfraction, wells were coated with the histone subfraction (as above), washed in PBS, then incubated for 3 h at 37°C with PLC in PLC buffer (2 units/ml), PLD in PLD buffer (8 units/ml), with control wells containing either PLD buffer or PBS. Following the digestion, all wells were washed in TBST, incubated in 0.5% casein/TBST (1hr, RT), incubated in 1H6 (1.0, 0.1, 0.01 µg/ml in casein/ TBST) for 2 h at RT. After extensive washing with TBST, reaction with HRP-anti-mouse IgG and further washing with TBST, the wells were assayed with OPD, as described above.

Immunoprecipitation and mass spectrometric analysis. Three full 15 cm dishes of NIH 3T3 cells were fractionated using the Qproteome Cell Compartment Kit (QIAGEN). Fraction 3 (Nuclear Proteins) was divided into two equal aliquots, pre-cleared by addition of normal mouse IgG, anti-mouse IgG, protein A/G sepharose beads and incubated ON at 4°C with continuous rotation. After centrifugation, the supernatants were incubated with either specific mAb or with normal mouse IgG and protein A/G sepharose, followed by rotation for 6 h at 4°C. The experiment was performed twice; once comparing 1H6 with IgG, and once comparing PL2-6 with IgG. After extensive washing, the immunoprecipitated pellets were reduced using trichloroethyl phosphine, alkylated (iodoacetamide), and digested with sequencing grade trypsin, as previously described.[32] Briefly, extracted peptides were analyzed via nanoscale liquid chromatography quadrupole-time-of-flight mass spectrometry using a FAMOS Ultimate nanoscale capillary LC (Dionex).

Following desalting (PepClean C18 column, Pierce), tryptic peptides were separated using a linear water/acetonitrile gradient (0.1% formic acid) on a Acclaim PepMap reversed-phase capillary column (3 µm, C18, 100 Angstrom pore size, 75 µm ID × 15 cm, 15 µm tip; LC Packings), with an inline PepMap 100 precolumn (C18, 300 µm ID × 5 mm; LC Packings) as a loading column. Mass spectrometry was conducted as previously described.[32,33] Peptides were eluted inline with a hybrid quadrupole time-of-flight mass spectrometer (QSTAR, MDSSCIEX) using a solvent gradient of 2–30% solvent B in 120 min and then 30–80% B in 10 min, in which solvent A is 0.1% formic acid and solvent B is 80% acetonitrile containing 0.1% formic acid. Data acquisition on the mass spectrometer was performed in information-dependent mode, whereby precursor peptides were automatically selected based on an MS-only scan and subjected to collision activated dissociation (MS/MS) in subsequent scans using a mass-dependent profile to set the collision energy for each MS/MS-interrogated peptide. Peak list generation, peptide mass fingerprint peak picking, and relative quantification and protein identification were performed with the ProteinPilotTM software (version 4.0; ABSciex). Default parameters were used for all analyses.

Protein searches were conducted using the UniProtKB/Swiss-Prot protein knowledgebase release 2011–03. MS/MS spectrum was searched against a database of human protein sequences using a mass tolerance of 0.6 Da and a detected protein threshold confidence of greater than 90%, set to detect contaminants (e.g., serum albumin). The number of unique proteins searched was 76,053. Threshold score for accepting individual MS/MS spectra was 95% confidence, based on confirmation by western blot analysis. Trypsin autolysis peaks and keratin tryptic peptides were known contaminants that were excluded from database searching. Peptide prevalence was estimated using the count of peptides for each protein that achieved $>$ 95% significance. The detected protein threshold was set to 2.0 to achieve 95% confidence as determined by the Paragon algorithm (Applied Biosystems) to minimize redundancy, as recently described[34,35] and using automated bias correction.

Disclosure of Potential Conflicts of Interest

No potential conflicts of interest were disclosed.

Acknowledgments

A.L.O. and D.E.O. were Visiting Scientists at the German Cancer Research Center (DKFZ, Heidelberg) in the laboratories of Peter Lichter and Harald Herrmann, and at MMCRI in the laboratory of I.P. I.P. was supported by grant HL35627 from NIH and a grant from the Maine Cancer Foundation, and institutional support from Maine Medical Center. C.P.H.V. was supported by NIH grant HL083151 and institutional support from the Maine Medical Center. Y.M. was supported by the DFG. This project was supported by the Protein, Nucleic Acid and Cell Imaging Core facility (I.P. and C.P.H.V.) of grant number P30RR030927/P30GM103392, Phase III COBRE in Vascular Biology (R. Friesel, P.I.), a grant supported by the National Center for Research Resources and the National Institute of General Medical Sciences. The authors thank M. Monestier (Temple University) for the gift of antibodies and helpful comments, and to L. Schermelleh (University of Oxford) and H. Leonhardt (Ludwig Maximilians University Munich) for generous assistance with 3-D SIM. K. Palczewski and D. Mustafi (Case Western Reserve University) generously provided an aliquot of mAb 4B6. Thanks are also extended to M. Cremer (LMU, Munich), M. Hergt (DKFZ) and A. Kirov (MMCRI).

Supplemental Material

Supplemental materials may be found here:
www.landesbioscience.com/journals/nucleus/article/19662/

References

1. Kramers K, Stemmer C, Monestier M, van Bruggen MC, Rijke-Schilder TP, Hylkema MN, et al. Specificity of monoclonal anti-nucleosome auto-antibodies derived from lupus mice. J Autoimmun 1996; 9:723-9; PMID: 9115574; http://dx.doi.org/10.1006/jaut.1996.0094
2. Olins AL, Langhans M, Monestier M, Schlotterer A, Robinson DG, Viotti C, et al. An epichromatin epitope: persistence in the cell cycle and conservation in evolution. Nucleus 2011; 2:47-60; PMID: 21647299; http://dx.doi.org/10.4161/nucl.2.1.13655
3. Leventis PA, Grinstein S. The distribution and function of phosphatidylserine in cellular membranes. Annu Rev Biophys 2010; 39:407-27; PMID:20192774; http://dx.doi.org/10.1146/annurev.biophys.093008.131234
4. Mourdjeva M, Kyurkchiev D, Mandinova A, Altankova I, Kehayov I, Kyurkchiev S. Dynamics of membrane translocation of phosphatidylserine during apoptosis detected by a monoclonal antibody. Apoptosis 2005; 10:209-17; PMID:15711937; http://dx.doi.org/10.1007/s10495-005-6076-5
5. Mandinov L, Mandinova A, Kyurkchiev S, Kyurkchiev D, Kehayov I, Kolev V, et al. Copper chelation represses the vascular response to injury. Proc Natl Acad Sci U S A 2003; 100:6700-5; PMID:12754378; http://dx.doi.org/10.1073/pnas.1231994100
6. Katadae M, Hagiwara K, Wada A, Ito M, Umeda M, Casey PJ, et al. Interacting targets of the farnesyl of transducin gamma-subunit. Biochemistry 2008; 47: 8424-33; PMID:18636747; http://dx.doi.org/10.1021/bi800359h
7. Calderon F, Kim HY. Detection of intracellular phosphatidylserine in living cells. J Neurochem 2008; 104:1271-9; PMID:18028336; http://dx.doi.org/10.1111/j.1471-4159.2007.05079.x
8. Schermelleh L, Carlton PM, Haase S, Shao L, Winoto L, Kner P, et al. Subdiffraction multicolor imaging of the nuclear periphery with 3D structured illumination microscopy. Science 2008; 320:1332-6; PMID: 18535242; http://dx.doi.org/10.1126/science.1156947
9. Malhas A, Goulbourne C, Vaux DJ. The nucleoplasmic reticulum: form and function. Trends Cell Biol 2011; 21:362-73; PMID:21514163; http://dx.doi.org/10.1016/j.tcb.2011.03.008
10. Robbins E, Pederson T, Klein P. Comparison of mitotic phenomena and effects induced by hypertonic solutions in HeLa cells. J Cell Biol 1970; 44:400-16; PMID:5411081; http://dx.doi.org/10.1083/jcb.44.2.400
11. Hancock R. Internal organisation of the nucleus: assembly of compartments by macromolecular crowding and the nuclear matrix model. Biol Cell 2004; 96:595-601; PMID:15519694; http://dx.doi.org/10.1016/j.biolcel.2004.05.003
12. Richter K, Nessling M, Lichter P. Experimental evidence for the influence of molecular crowding on nuclear architecture. J Cell Sci 2007; 120:1673-80; PMID:17430977; http://dx.doi.org/10.1242/jcs.03440
13. Ohlenbusch HH, Olivera BM, Tuan D, Davidson N. Selective dissociation of histones from calf thymus nucleoprotein. J Mol Biol 1967; 25:299-315; PMID: 4291873; http://dx.doi.org/10.1016/0022-2836(67)90143-X
14. Shechter D, Dormann HL, Allis CD, Hake SB. Extraction, purification and analysis of histones. Nat Protoc 2007; 2:1445-57; PMID:17545981; http://dx.doi.org/10.1038/nprot.2007.202
15. Waga S, Tan EM, Rubin RL. Identification and isolation of soluble histones from bovine milk and serum. Biochem J 1987; 244:675-82; PMID:3446184
16. Jensen RG. The composition of bovine milk lipids: January 1995 to December 2000. J Dairy Sci 2002; 85:295-350; PMID:11913692; http://dx.doi.org/10.3168/jds.S0022-0302(02)74079-4
17. Rodriguez-Collazo P, Leuba SH, Zlatanova J. Robust methods for purification of histones from cultured mammalian cells with the preservation of their native modifications. Nucleic Acids Res 2009; 37:e81; PMID: 19443446; http://dx.doi.org/10.1093/nar/gkp273
18. Losman MJ, Fasy TM, Novick KE, Monestier M. Monoclonal autoantibodies to subnucleosomes from a MRL/Mp(-)+/+ mouse. Oligoclonality of the antibody response and recognition of a determinant composed of histones H2A, H2B, and DNA. J Immunol 1992; 148:1561-9; PMID:1371530
19. Cocco L, Gilmour RS, Papa S, Capitani S, Manzoli FA. Response of isolated nuclei to phospholipid vesicles: analysis of chromatin sensitivity to DNase I and micrococcal nuclease. Cell Biol Int Rep 1984; 8:55-63; PMID:6231116; http://dx.doi.org/10.1016/0309-1651(84)90182-6
20. Capitani S, Cocco L, Matteucci A, Caramelli E, Papa S, Manzoli FA. Response of isolated nuclei to phospholipid vesicles: analysis of the nuclear proteins after treatment with phosphatidylserine and phosphatidylcholine and comparison with heparin. Cell Biol Int Rep 1984; 8:289-96; PMID:6733788; http://dx.doi.org/10.1016/0309-1651(84)90155-3
21. Capitani S, Caramelli E, Felaco M, Miscia S, Manzoli FA. Effect of phospholipid vesicles on endogenous RNA polymerase activity of isolated rat liver nuclei. Physiol Chem Phys 1981; 13:153-8; PMID:6169101
22. Pereira LF, Marco FM, Boimorto R, Caturla A, Bustos A, De la Concha EG, et al. Histones interact with anionic phospholipids with high avidity; its relevance for the binding of histone-antihistone immune complexes. Clin Exp Immunol 1994; 97:175-80; PMID: 8050163; http://dx.doi.org/10.1111/j.1365-2249.1994.tb06064.x
23. Fürnrohr BG, Groer GJ, Sehnert B, Herrmann M, Voll RE. Interaction of histones with phospholipids–implications for the exposure of histones on apoptotic cells. Autoimmunity 2007; 40:322-6; PMID:17516219; http://dx.doi.org/10.1080/08916930701356457
24. Das R, Plow EF. Phosphatidylserine as an anchor for plasminogen and its plasminogen receptor, histone H2B, to the macrophage surface. J Thromb Haemost 2011; 9:339-49; PMID:21040449; http://dx.doi.org/10.1111/j.1538-7836.2010.04132.x
25. Radic M, Marion T, Monestier M. Nucleosomes are exposed at the cell surface in apoptosis. J Immunol 2004; 172:6692-700; PMID:15153485
26. van Meer G, Voelker DR, Feigenson GW. Membrane lipids: where they are and how they behave. Nat Rev Mol Cell Biol 2008; 9:112-24; PMID:18216768; http://dx.doi.org/10.1038/nrm2330
27. Fairn GD, Schieber NL, Ariotti N, Murphy S, Kuerschner L, Webb RI, et al. High-resolution mapping reveals topologically distinct cellular pools of phosphatidylserine. J Cell Biol 2011; 194:257-75; PMID: 21788369; http://dx.doi.org/10.1083/jcb.201012028
28. Maneta-Peyret L, Compère P, Moreau P, Goffinet G, Cassagne C. Immunocytochemistry of lipids: chemical fixatives have dramatic effects on the preservation of tissue lipids. Histochem J 1999; 31:541-7; PMID:10507461; http://dx.doi.org/10.1023/A:1003844107756
29. Güttinger S, Laurell E, Kutay U. Orchestrating nuclear envelope disassembly and reassembly during mitosis. Nat Rev Mol Cell Biol 2009; 10:178-91; PMID: 19234477; http://dx.doi.org/10.1038/nrm2641
30. Hetzer MW. The nuclear envelope. Cold Spring Harb Perspect Biol 2010; 2:a000539; PMID:20300205; http://dx.doi.org/10.1101/cshperspect.a000539
31. Mustafi D, Kevany BM, Genoud C, Okano K, Cideciyan AV, Sumaroka A, et al. Defective photoreceptor phagocytosis in a mouse model of enhanced S-cone syndrome causes progressive retinal degeneration. FASEB J 2011; 25:3157-76; PMID:21659555; http://dx.doi.org/10.1096/fj.11-186767
32. Romero D, O'Neill C, Terzic A, Contois L, Young K, Conley BA, et al. Endoglin regulates cancer-stromal cell interactions in prostate tumors. Cancer Res 2011; 71:3482-93; PMID:21444673; http://dx.doi.org/10.1158/0008-5472.CAN-10-2665
33. Koleva RI, Conley BA, Romero D, Riley KS, Marto JA, Lux A, et al. Endoglin structure and function: Determinants of endoglin phosphorylation by transforming growth factor-beta receptors. J Biol Chem 2006; 281: 25110-23; PMID:16785228; http://dx.doi.org/10.1074/jbc.M601288200
34. Ruppen I, Grau L, Orenes-Piñero E, Ashman K, Gil M, Algaba F, et al. Differential protein expression profiling by iTRAQ-two-dimensional LC-MS/MS of human bladder cancer EJ138 cells transfected with the metastasis suppressor KiSS-1 gene. Mol Cell Proteomics 2010; 9:2276-91; PMID:20139371; http://dx.doi.org/10.1074/mcp.M900255-MCP200
35. Shilov IV, Seymour SL, Patel AA, Loboda A, Tang WH, Keating SP, et al. The Paragon Algorithm, a next generation search engine that uses sequence temperature values and feature probabilities to identify peptides from tandem mass spectra. Mol Cell Proteomics 2007; 6:1638-55; PMID:17533153; http://dx.doi.org/10.1074/mcp.T600050-MCP200